

Supporting Information

Nitrodopamine Modified MnO₂ NS-MoS₂ QDs Hybrid Nanocomposite for Extra- and Intracellular Detection of Glutathione

Gomathi Sivakumar,^a Ajay Gupta,^b Anashwara Babu,^a Pijus K. Sasmal,*^b Samarendra Maji*^a

^aDepartment of Chemistry, Faculty of Engineering and Technology, SRM Institute of Science and Technology (SRMIST), Kattankulathur, Tamil Nadu-603203, India. Corresponding author E-mail: samarenr@srmist.edu.in

^bSchool of Physical Sciences, Jawaharlal Nehru University, New Delhi-110-067, India. Corresponding author E-mail: pijus@mail.jnu.ac.in

Table S1. The crystallite size of the designed pure MnO₂ NS and surface-modified ND@MnO₂ NS and DA@MnO₂ NS.

S. No	(hkl)	MnO ₂ NS			ND@MnO ₂ NS			DA@MnO ₂ NS		
		2θ (°)	FWHM (β)	Crystallite Size (nm)	2θ (°)	FWHM (β)	Crystallite Size (nm)	2θ (°)	FWHM (β)	Crystallite Size (nm)
1	(001)	12.29°	4.5933	1.82	14.22°	9.5439	0.88	14.8°	4.3958	1.90
2	(002)	18.54°	7.0156	1.2	18.74°	12.8279	0.66	18.97°	9.111	0.92
3	(110)	36.39°	21.2331	0.41	37.25°	15.2853	0.57	37.01°	28.1328	0.31
4	(020)	65.66°	431.3521	0.02	65.87°	258.092	0.04	65.55°	233.04	0.04
Average			0.86	Average			0.54	Average		

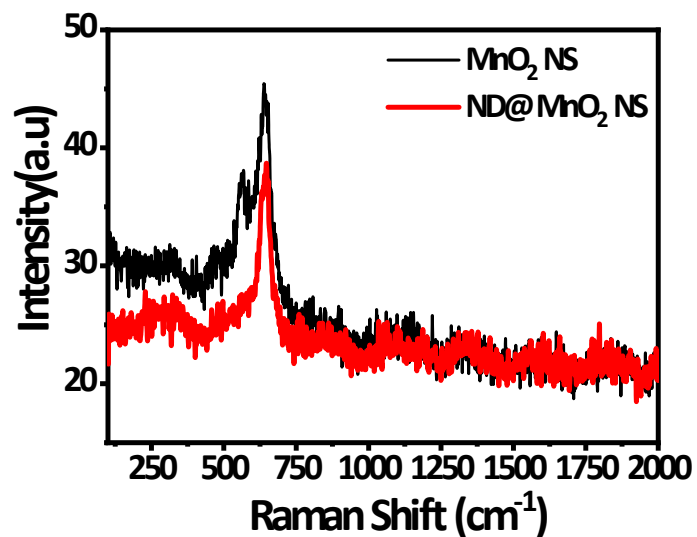


Figure S1. Raman spectrum of a) MnO₂ NS, and b) ND@MnO₂ NS.

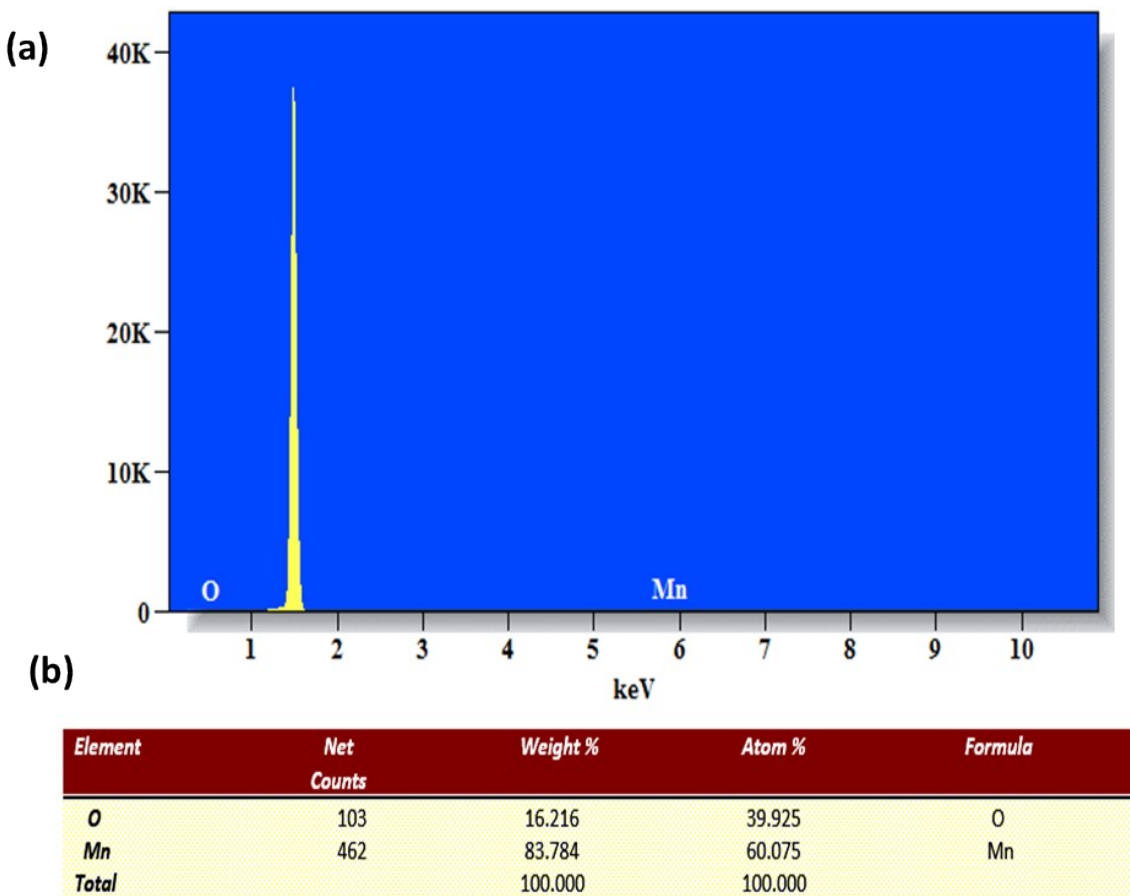


Figure S2. a) EDX data of MnO_2 NS, and b) quantitative weight percentage data of elements present in the MnO_2 NS.

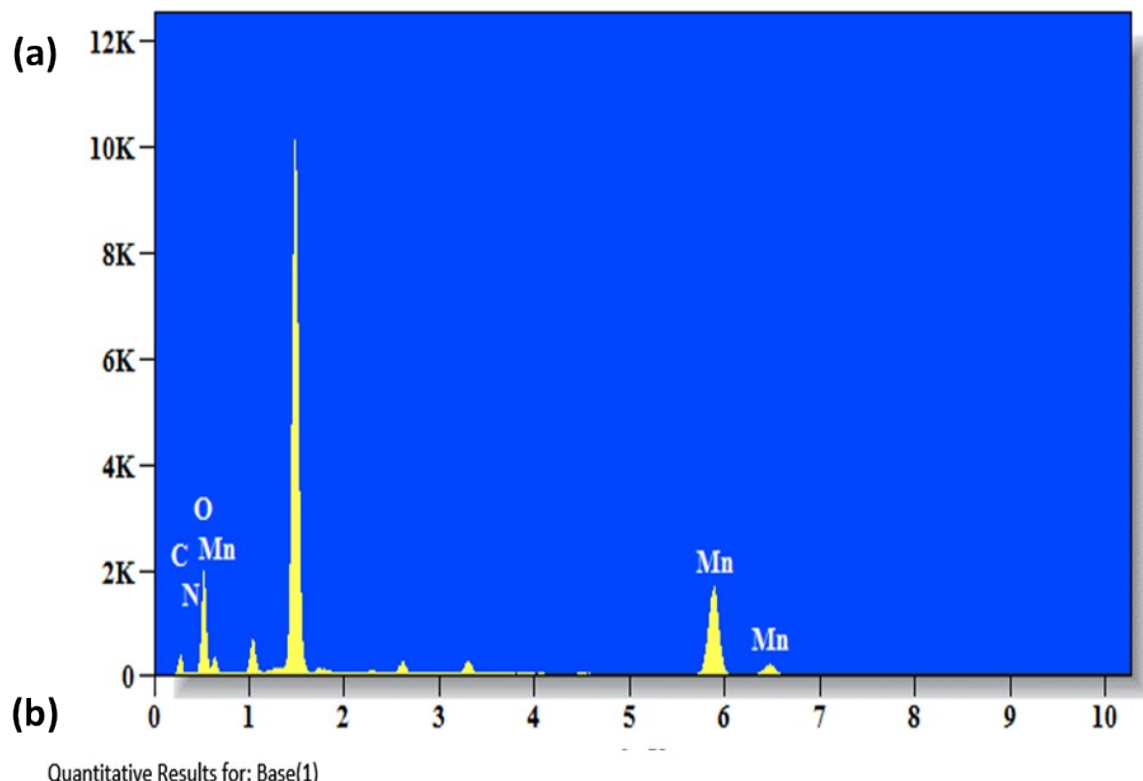


Figure S3. a) EDX data of ND@MnO₂ NS, and b) quantitative weight percentage data of elements present in the ND@MnO₂ NS.

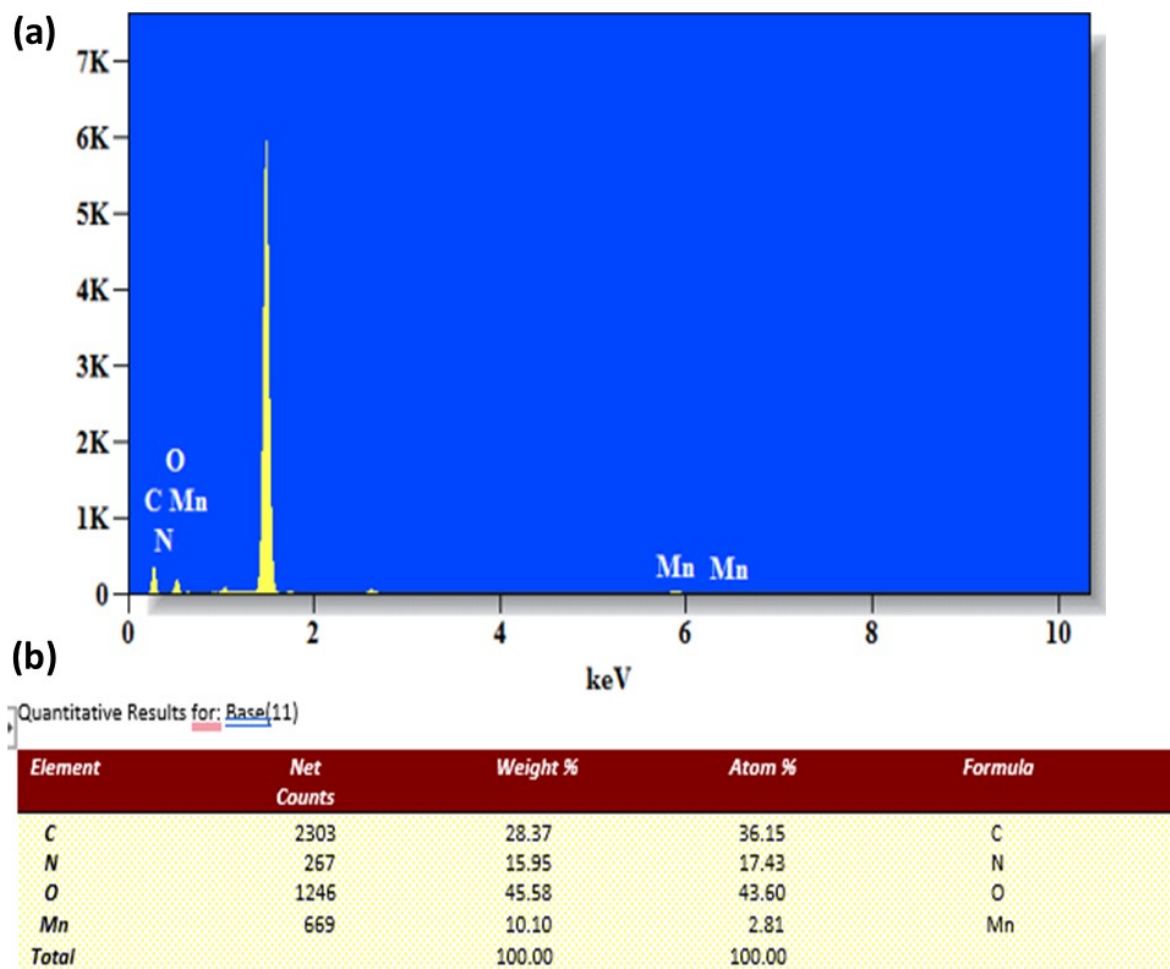


Figure S4. a) EDX data of DA@MnO₂ NS, and b) quantitative weight percentage data of elements present in the DA@MnO₂ NS.

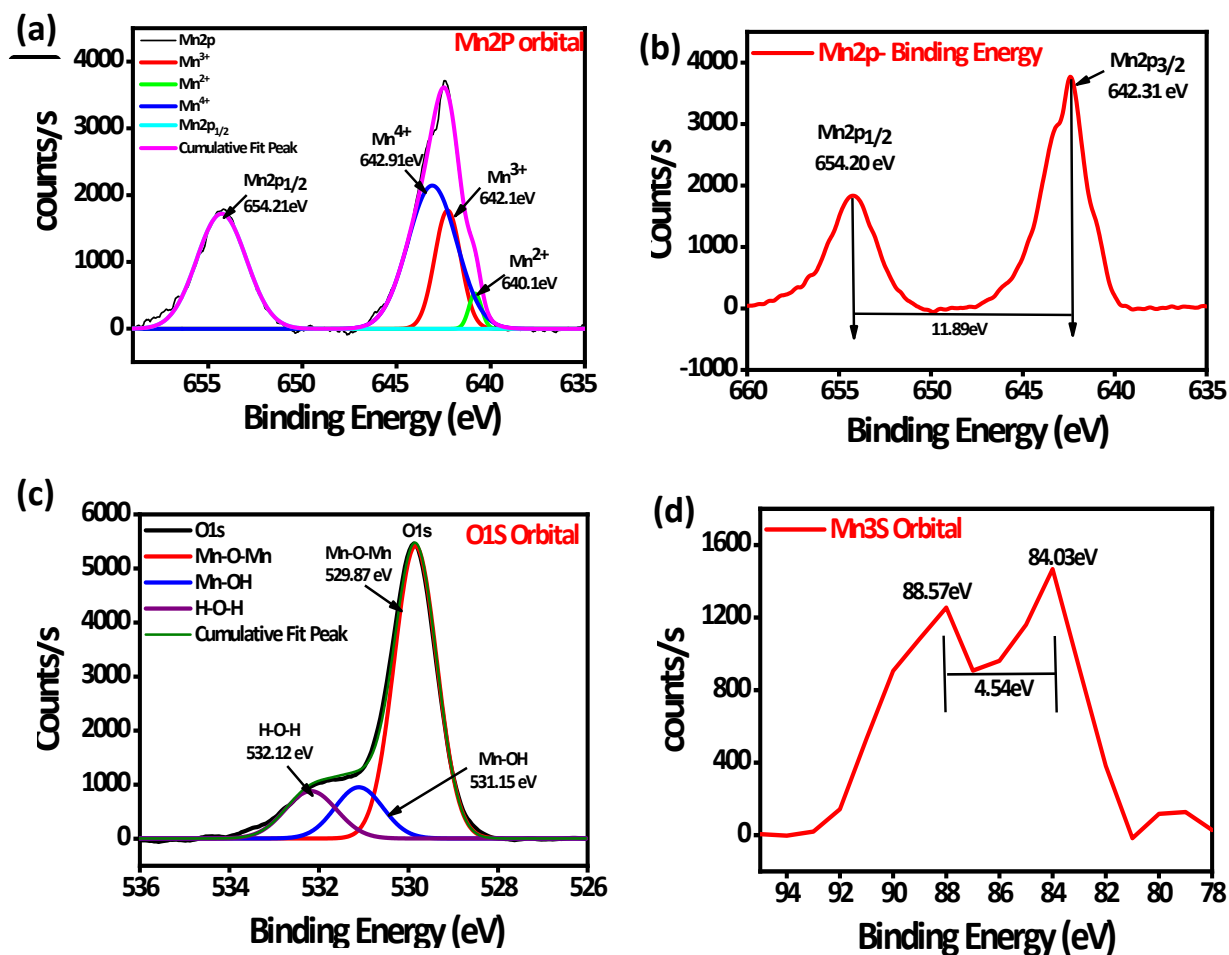


Figure S5. XPS spectra recorded from the MnO₂ NS; XPS spectra of a) Mn2p, b) Mn2P binding energy, and c) O1s orbital d) Mn3s orbital.

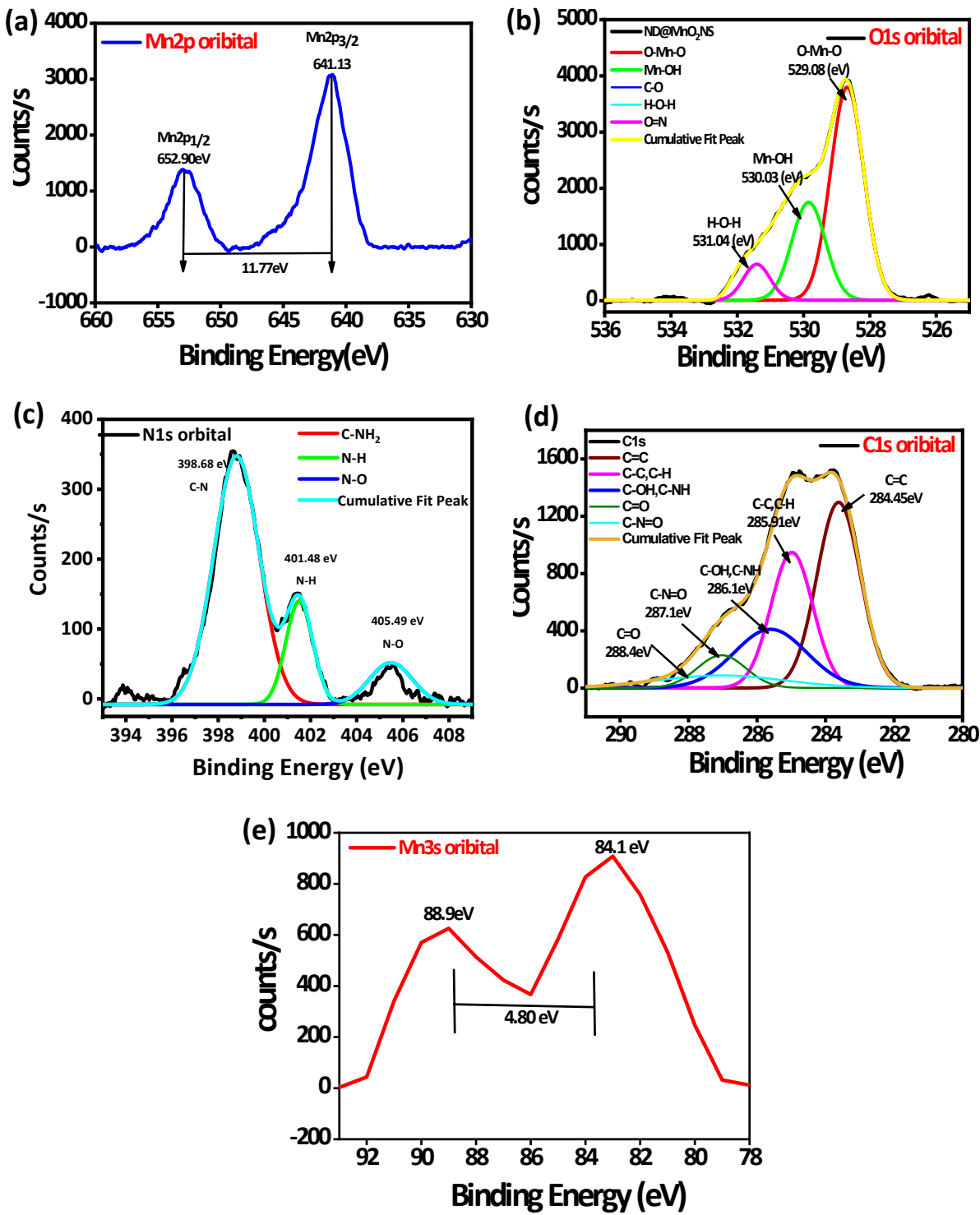


Figure S6. XPS spectra recorded from the ND@MnO₂ NS; XPS spectra of a) Mn2p, b) O1s, c) N1s, d) C1s, and e) Mn3s deconvolution spectra.

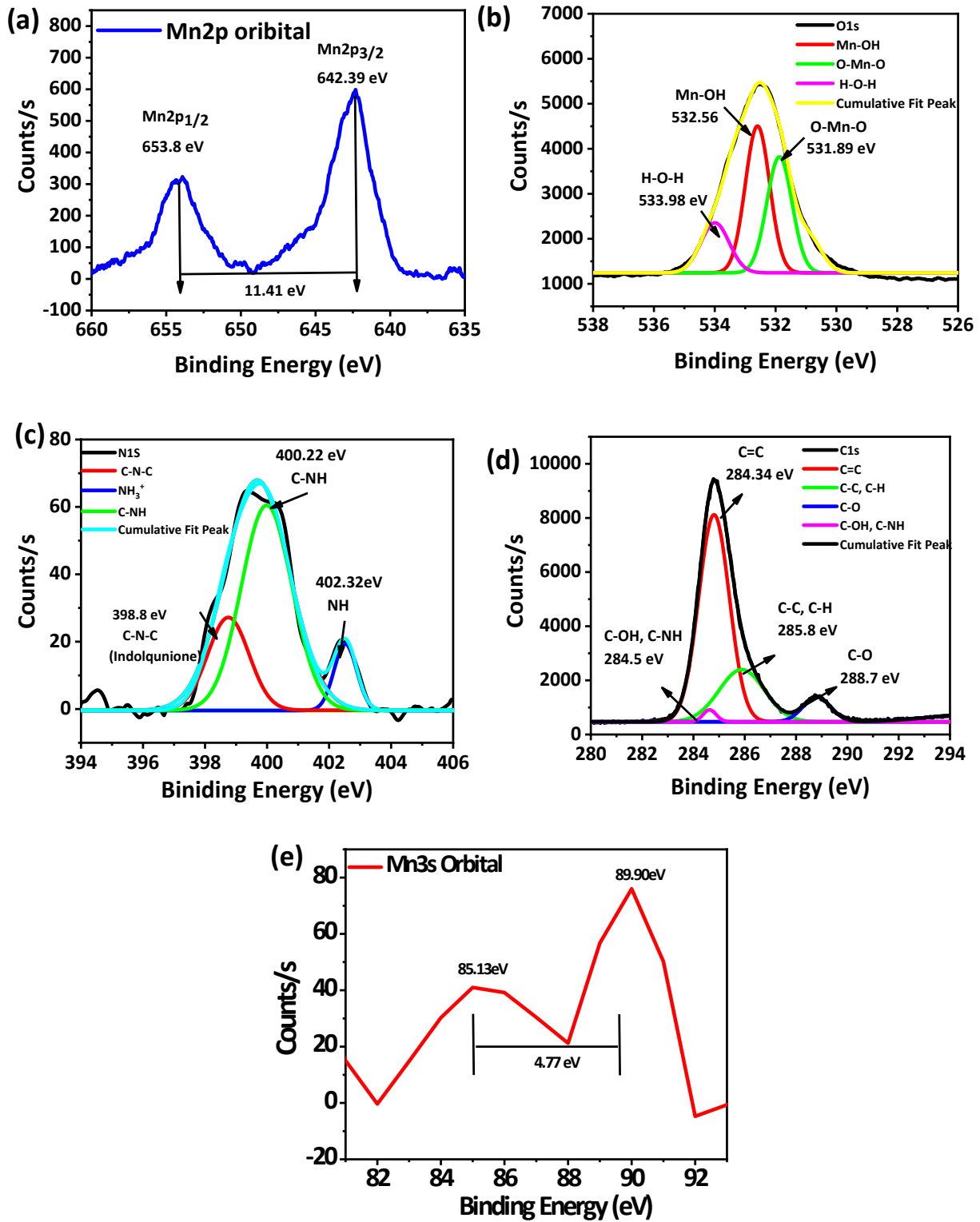
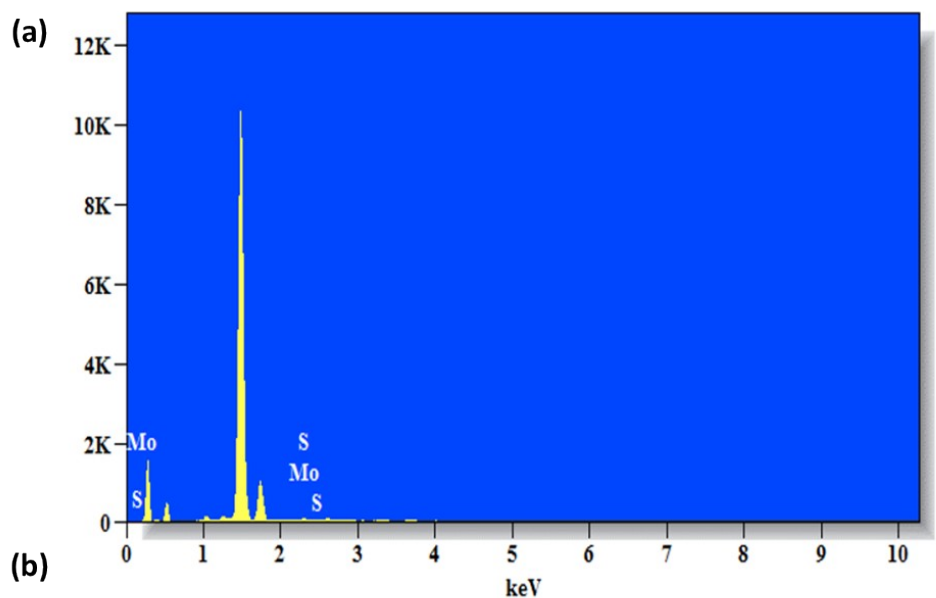


Figure S7. XPS spectra recorded from the DA@MnO₂ NS; XPS spectra of a) Mn2p, b) O1s, c) N1s, d) C1s, and e) Mn3s deconvolution spectra.



Quantitative Results for: Base(2)

Element	Net Counts	Weight %	Atom %	Formula
S	685	37.695	64.419	S
Mo	675	62.305	35.581	Mo
Total		100.000	100.000	

Figure S8. a) EDX data of MoS₂ QDs, and b) quantitative weight percentage data of elements present in the MoS₂ QDs.

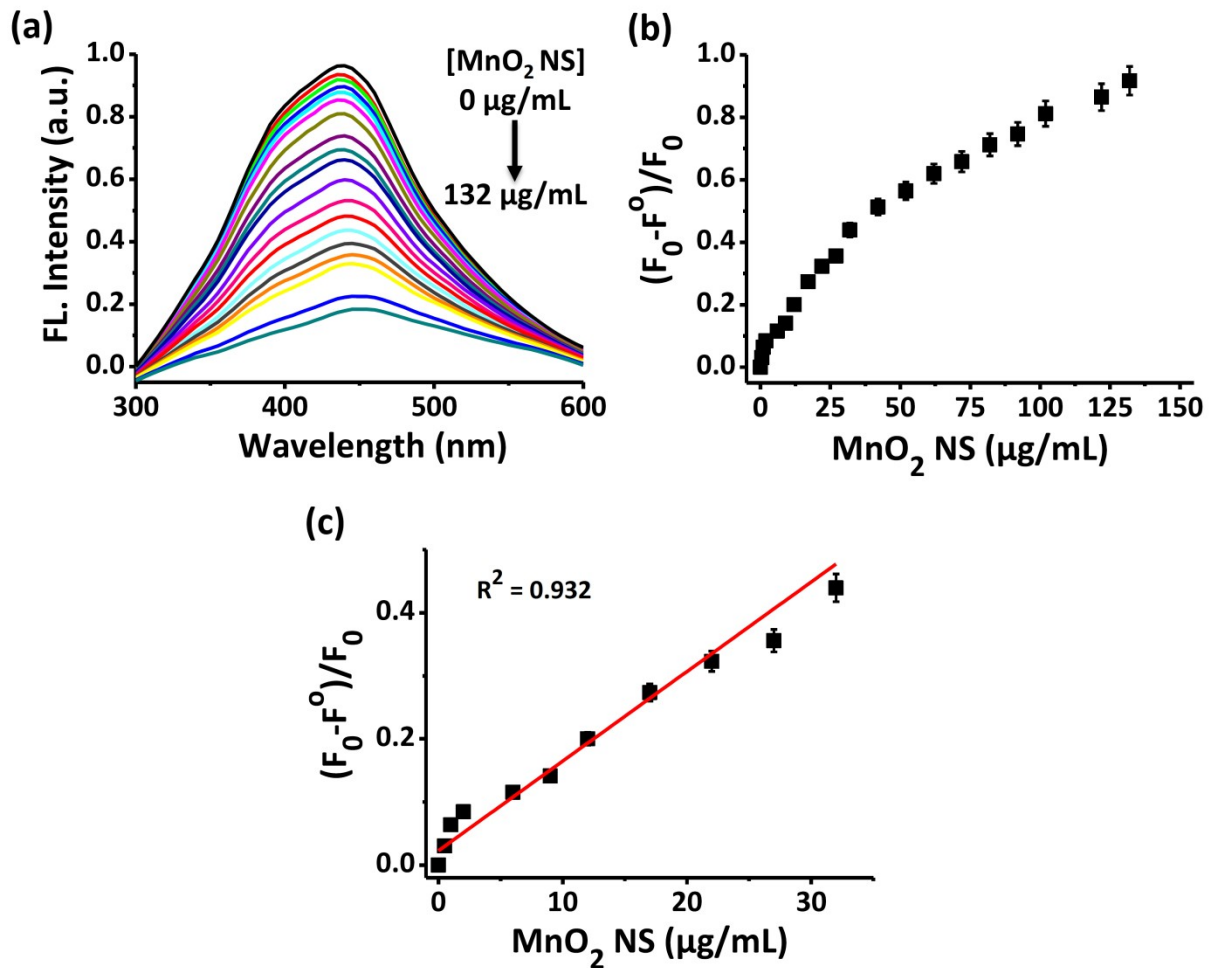


Figure S9. a) Fluorescence spectra of MoS₂ QDs (100 µg/mL) in 1:10 DMF/PBS (1X, pH 7.4) with different concentrations of MnO₂ NS (0-132 µg/mL). The emission spectra of MoS₂ QDs ($\lambda_{\text{ex}} = 275$ nm and $\lambda_{\text{em}} = 435$ nm) were recorded just after each addition of MnO₂ NS. b) The kinetic curve at λ_{em} 435 nm for the change in fluorescence intensity ratio with different MnO₂ NS concentrations. c) Relationship between quenching efficiency and the concentrations of MnO₂ NS. F° and F_0 are fluorescence intensities of MoS₂ QDs in the presence and absence of MnO₂ NS, respectively.

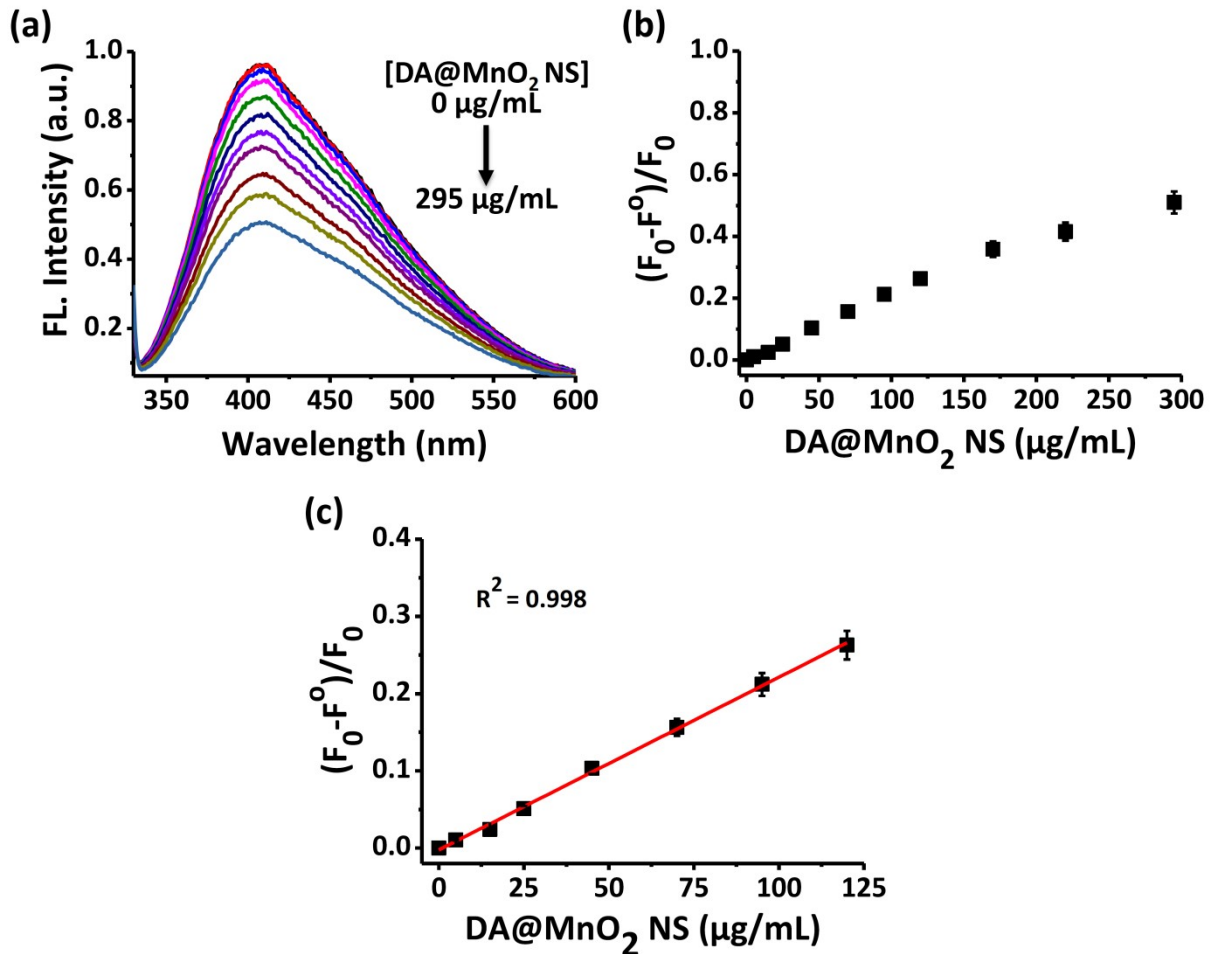


Figure S10. a) Fluorescence spectra of MoS₂ QDs (100 μg/mL) in 1:10 DMF/PBS (1X, pH 7.4) with different concentrations of DA@MnO₂ NS (0-295 μg/mL). The emission spectra of MoS₂ QDs ($\lambda_{\text{ex}} = 275$ nm and $\lambda_{\text{em}} = 435$ nm) were recorded just after each addition of DA@MnO₂ NS. b) Kinetic curve at λ_{em} 435 nm for the change in fluorescence intensity ratio with different DA@MnO₂ NS concentrations. c) Relationship between quenching efficiency and the concentrations of DA@MnO₂ NS. F^o and F_0 are fluorescence intensities of MoS₂ QDs in the presence and absence of DA@MnO₂ NS, respectively.

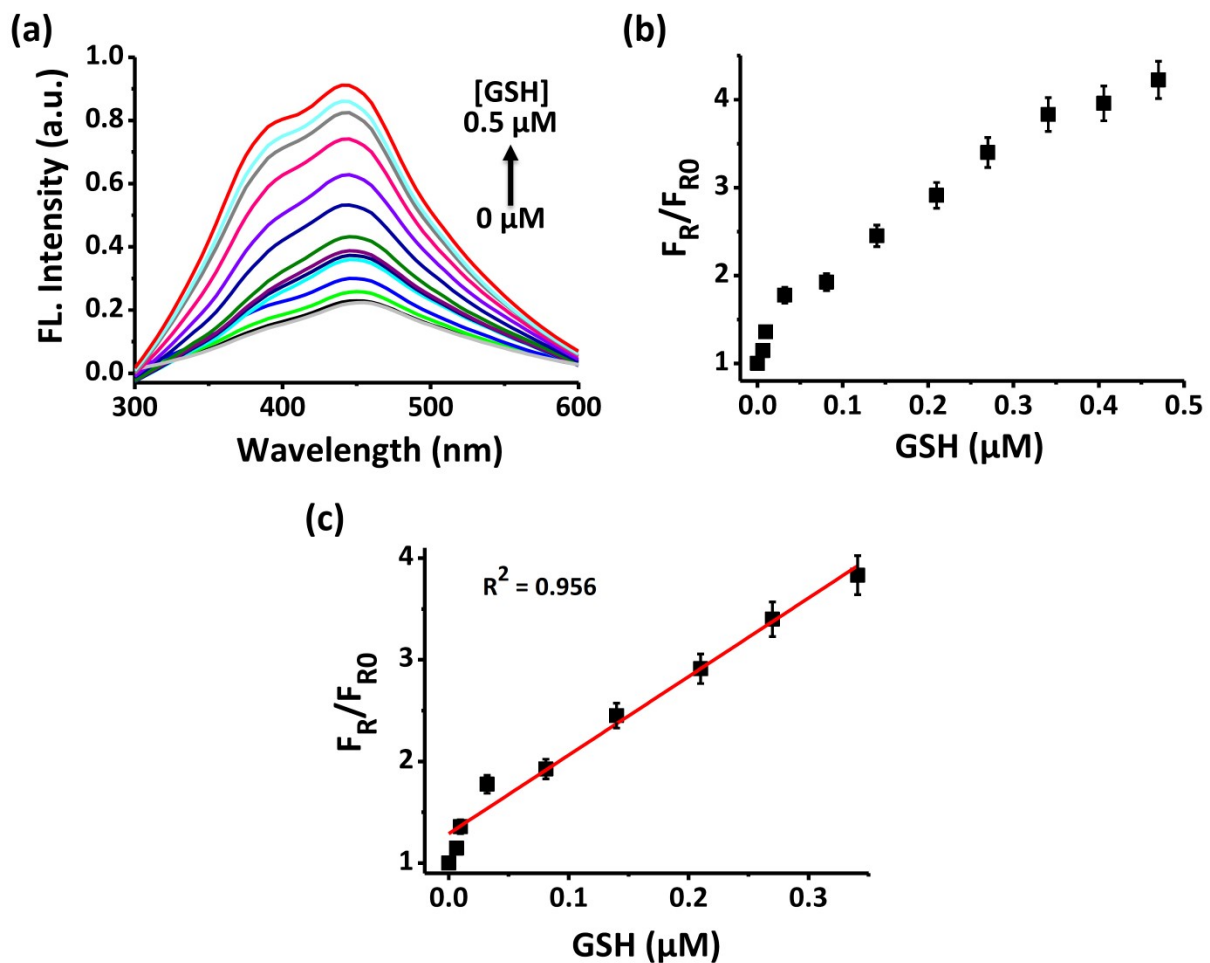


Figure S11. a) Fluorescence spectra of MnO_2 NS@ MoS_2 QDs composite in 1:10 DMF/PBS (1X, pH 7.4) with different concentrations of GSH (0-0.5 μM). The emission spectra of MnO_2 NS@ MoS_2 QDs ($\lambda_{\text{ex}} = 275 \text{ nm}$ and $\lambda_{\text{em}} = 435 \text{ nm}$) were recorded just after each addition of GSH. b) Kinetic curve at λ_{em} 435 nm for the change in fluorescence intensity ratio with different GSH concentrations. c) Relationship between fluorescence intensity ratio and the concentrations of GSH. F_R and F_{R0} are fluorescence intensities of MnO_2 NS@ MoS_2 QDs sensing probe in the presence and absence of GSH, respectively.

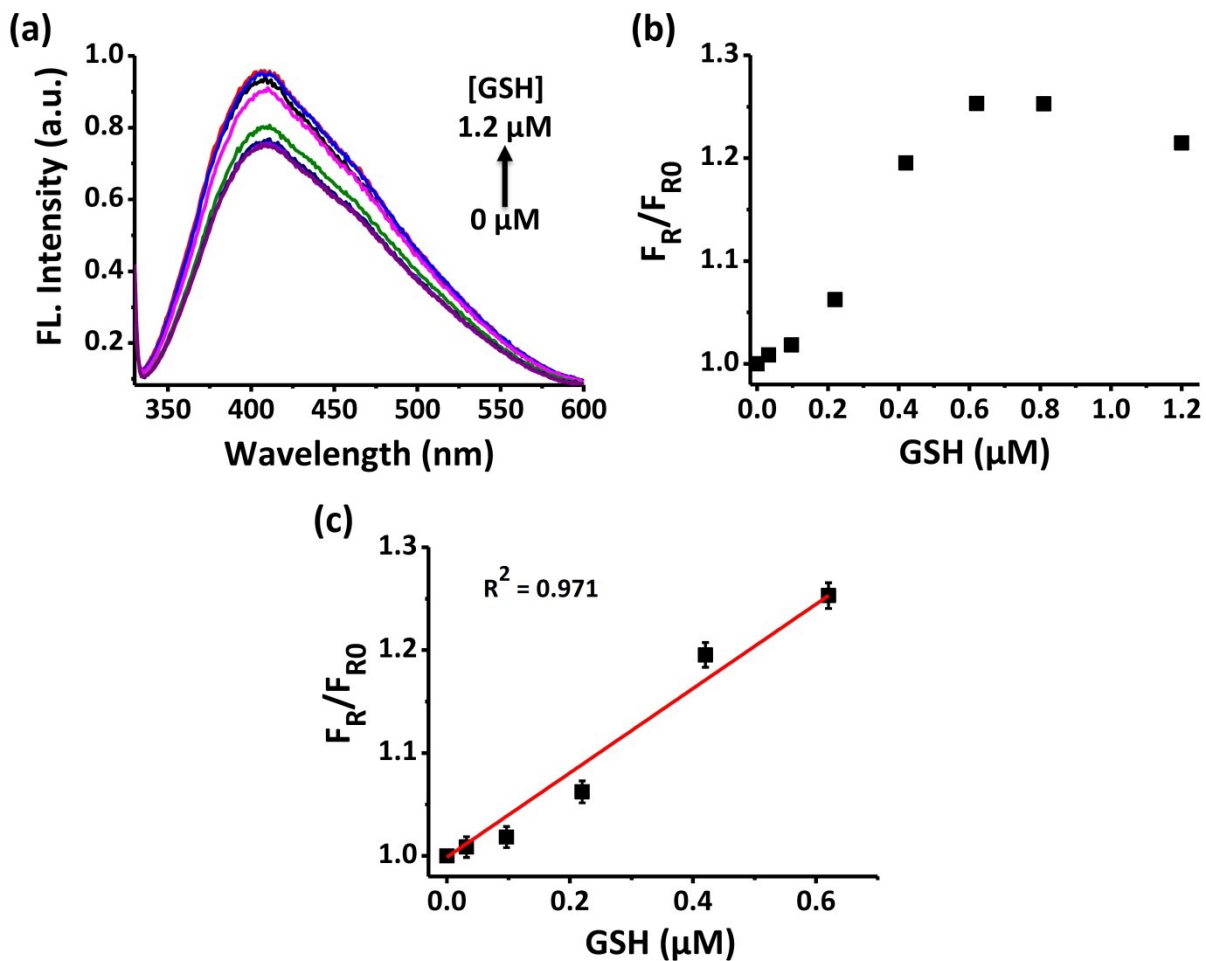


Figure S12. a) Fluorescence spectra of DA@MnO₂ NS@MoS₂ QDs composite in 1:10 DMF/PBS (1X, pH 7.4) with different concentrations of GSH (0-1.2 μM). The emission spectra of DA@MnO₂ NS@MoS₂ QDs ($\lambda_{\text{ex}} = 275 \text{ nm}$ and $\lambda_{\text{em}} = 435 \text{ nm}$) were recorded just after each addition of GSH. b) Kinetic curve at λ_{em} 435 nm for the change in fluorescence intensity ratio with different GSH concentrations. c) Relationship between fluorescence intensity ratio and the concentrations of GSH. F_R and F_{R0} are fluorescence intensities of DA@MnO₂ NS@MoS₂ QDs sensing probe in the presence and absence of GSH, respectively.

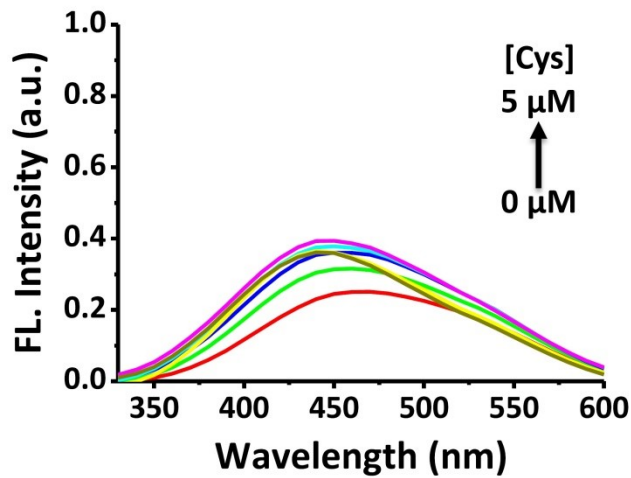


Figure S13. Fluorescence spectra of probe composite (DA@MnO₂ NS@MoS₂ QDs) in 1:10 DMF/PBS (1X, pH 7.4) with different concentrations of Cys (0-5 μM). The emission spectra of probe ($\lambda_{\text{ex}} = 275 \text{ nm}$ and $\lambda_{\text{em}} = 435 \text{ nm}$) were recorded just after each addition of Cys.

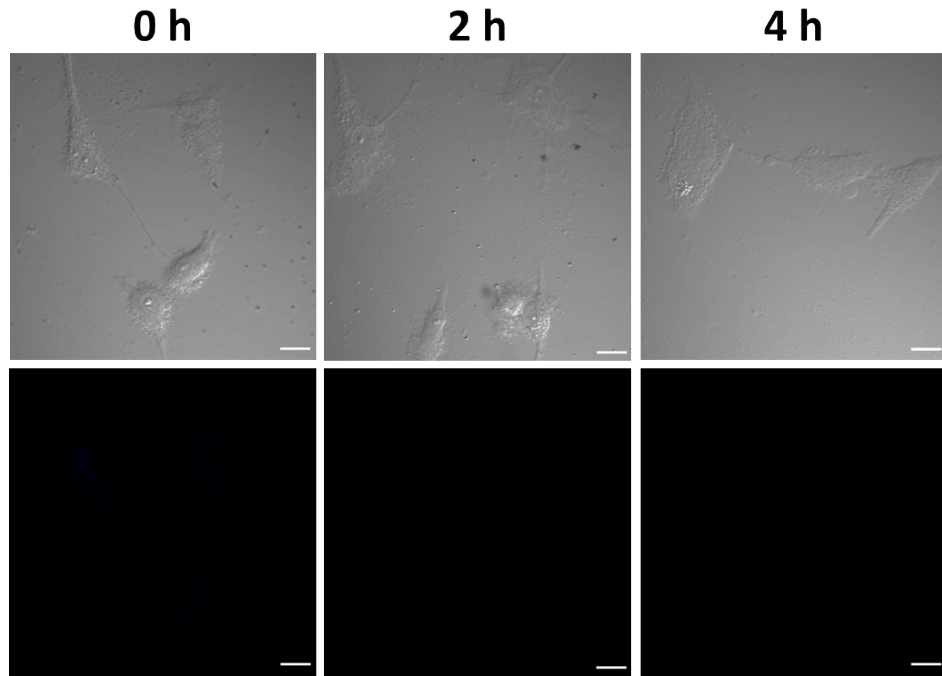


Figure S14. Confocal microscopy images of A549 cells incubated with ND@MnO₂ NS (50 μg/mL) for different time points. Top panels: under bright-field and bottom panels: under fluorescence modes. Scale bar = 10 μm.

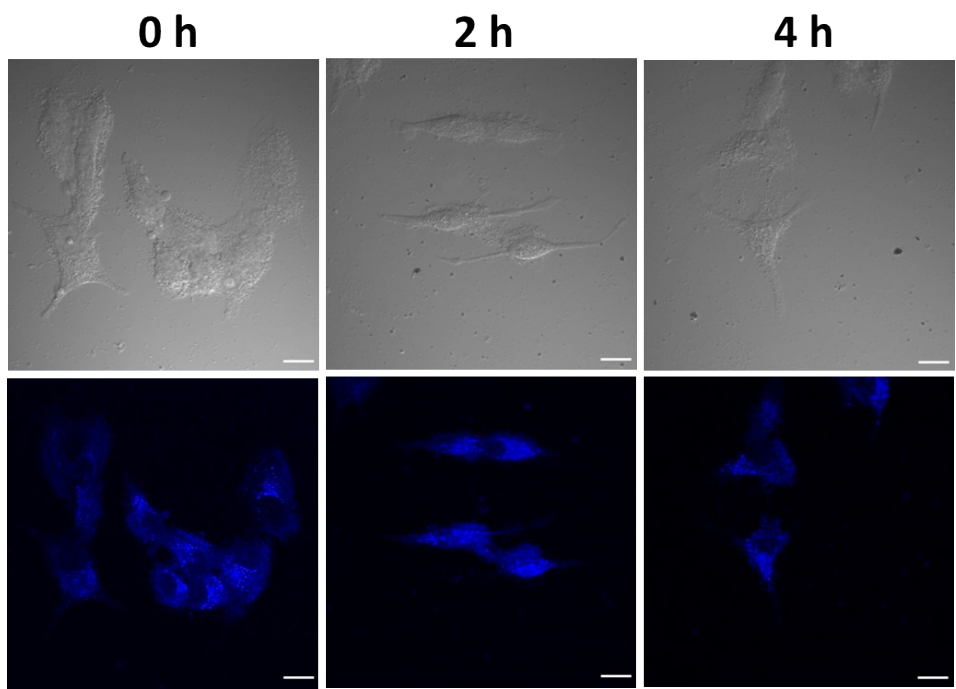


Figure S15. Confocal microscopy images of A549 cells incubated with MoS₂ QDs (50 µg/mL) for different time points. Top panels: under bright-field and bottom panels: under fluorescence modes. Scale bar = 10 µm.

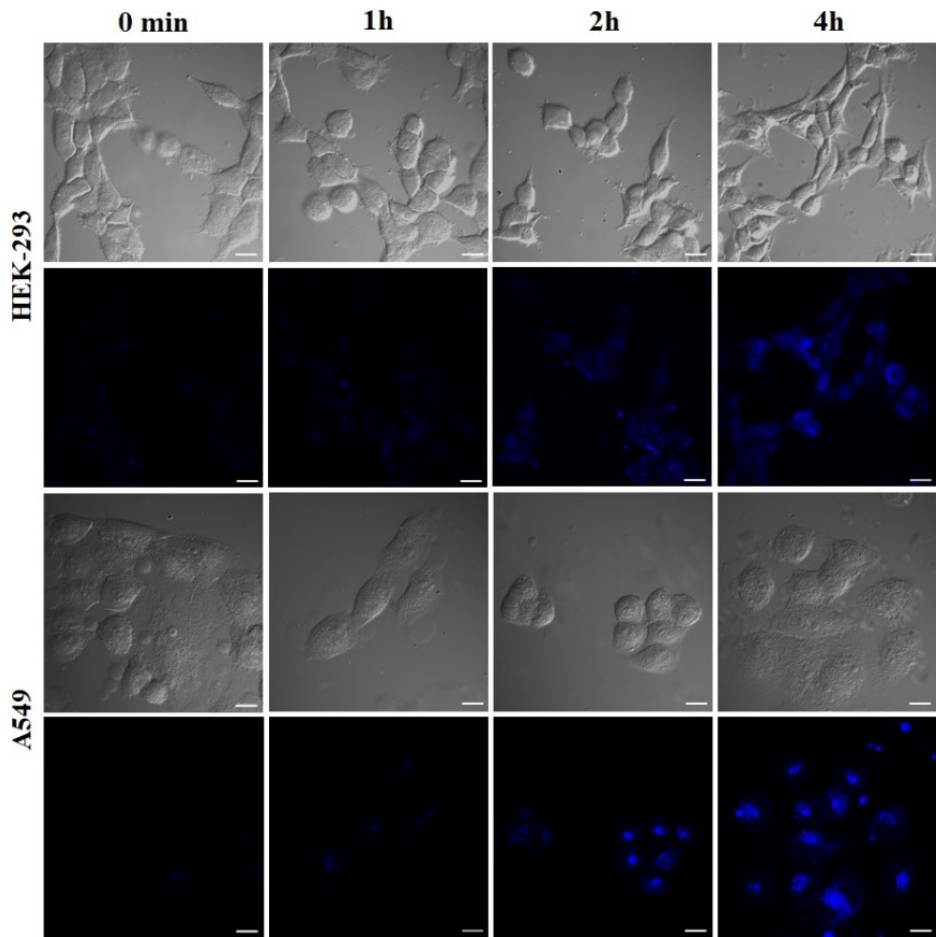


Figure S16. Confocal microscopy images of HEK293 and A549 cells incubated with probe (ND@MnO₂ NS@MoS₂ QDs) (50 µg/mL) for different time points under bright-field and fluorescence modes. Scale bar = 10 µm.